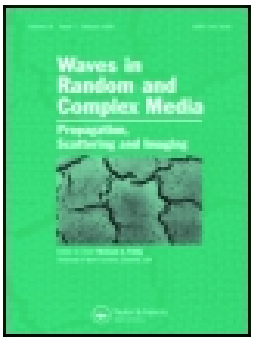

Waves in Random and Complex Media

ISSN: 1745-5030 (Print) 1745-5049 (Online) Journal homepage: http://www.tandfonline.com/loi/twrm20

Generation of infinitely long phase screens for modeling of optical wave propagation in atmospheric turbulence

A. M. Vorontsov , P. V. Paramonov , M. T. Valley & M. A. Vorontsov

Waves in Random and Complex Media
Vol. 18, No. 1, February 2008, 91–108

Generation of infinitely long phase screens for modeling of optical wave propagation in atmospheric turbulence

A. M. VORONTSOV†, P. V. PARAMONOV†, M. T. VALLEY‡ and M. A. VORONTSOV†‡*

†M.V. Lomonosov's Moscow State University, Leninskie Gory, Moscow, Russia
‡Sandia National Laboratories, 1515 Eubank Blvd. S..E. 87185-1139, New Mexico, Albuquerque, USA
†‡Army Research Laboratory, 2800 Powder Mill Rd., Adelphi, MD, 20783 and University of Maryland, College Park

(Received 27 January 2007; in final form 1 May 2007)

Numerical modeling of optical wave propagation in atmospheric turbulence is traditionally performed by using the so-called 'split'-operator method, where the influence of the propagation medium's refractive index inhomogeneities is accounted for only within a set of infinitely narrow phase distorting layers (phase screens). These phase screens are generated on a numerical grid of finite size, which corresponds to a rather narrow slice (spatial area) of atmospheric turbulence. In several important applications including laser target tracking, remote sensing, adaptive optics, and atmospheric imaging, optical system performance depends on atmospheric turbulence within an extended area that significantly exceeds the area associated with the numerical grid.

In this paper we discuss methods that allow the generation of a family of long (including infinitely long) phase screens representing an extended (in one direction) area of atmospheric turbulence-induced phase distortions. This technique also allows the generation of long phase screens with spatially inhomogeneous statistical characteristics.

1. Introduction

Random fluctuations in refractive index caused by air turbulent motion result in distortions of the optical waves as they propagate through the Earth's atmosphere. The influence of atmospheric turbulence on optical wave propagation is commonly described by either the stochastic equation for the field complex amplitude or the corresponding equation for its statistical moments [1–3]. In numerical analysis of these equations the refractive index fluctuations are typically represented as a sequence of statistically independent thin phase distorting layers (phase screens) separated by an optically homogeneous medium (layered phase distorting medium model) [4–8]. The phase screen approach is widely used for analysis of various atmospheric optics problems including laser beam propagation, remote sensing and imaging.

Numerical representation of a random phase screen is commonly performed inside a finite domain associated with the used numerical grid [9–12]. This bounded phase screen model is

*Corresponding author. E-mail: mvoronts@umd.edu

Waves in Random and Complex Media
ISSN: 1745-5030 (print), 1745-5049 (online)
http://www.tandf.co.uk/journals
DOI: 10.1080/17455030701429962

typically sufficient for the analysis of wave propagation along a fixed direction (optical axis) in 'frozen' turbulence.

In many practical applications including laser tracking of moving objects or laser object illumination from a moving platform, wave propagation occurs under conditions of continuously changing optical axis direction and/or its displacement. This requires consideration of a large region of turbulence that significantly exceeds the numerical grid size used for wave propagation analysis. Phase screen boundedness is also a problem for numerical analysis of wave propagation in moving turbulence [13].

In this paper we describe mathematical methods that can be used for numerical generation of non-periodic phase screens of arbitrary length (including infinite phase screens) with predefined statistical characteristics. The theoretical basis of phase screen generation methods is discussed in Section 2. In Section 3, this general analysis is applied for random phase screen generation in squares and extended rectangles. In Section 4, we present a 'screen-splicing' method that allows an extension of the phase screen generation domain to half-bands. In this section we also provide error estimation as well as the present algorithm for numerical implementation of the extended phase screen methods. Finally, in Section 4 we discuss modeling of infinitely extended random phase screens with statistical characteristics which are changing along a direction orthogonal to wave propagation.

2. Phase screen approach

Consider optical wave propagation along the Oz axis in the Cartesian coordinate system $Oxyz$, with $\vec{\rho} = (x, y, z)$ as a vector. Assume that the optical transmitter is located at the coordinate origin (0, 0, 0) and the receiver is located at the point $(0, 0, L)$ as shown in figure 1.

Propagation of the linear polarized monochromatic optical waves with complex amplitude $U(\vec{\rho}, t) = U(\vec{r}, z, t)$ through an optically inhomogeneous medium is commonly described by the following equation [14]

$$2ik\frac{\partial U(\vec{r}, z, t)}{\partial z} = \nabla_{\perp}^2 U(\vec{r}, z, t) + 2k^2 n(\vec{r}, z, t) U(\vec{r}, z, t), \quad \vec{r} = (x, y), \ t \geq 0. \tag{1}$$

Here k is the wavenumber, $\nabla_{\perp}^2 = \frac{\partial^2}{\partial x^2} + \frac{\partial^2}{\partial y^2}$, and $n(\vec{r}, z, t) = n(\vec{\rho}, t)$ is a random function corresponding to the refractive index fluctuations having zero mean value $\langle n(\vec{\rho}, t)\rangle = 0$. The notation $\langle\rangle$ is used to describe statistical averaging over the ensemble of refractive index realizations. The boundary conditions for U at the plane $z = 0$ are defined as

$$U(\vec{r}, z = 0, t) = U_0(\vec{r}),$$

where $U_0(\vec{r})$ is the optical field complex amplitude at the transmitter plane.

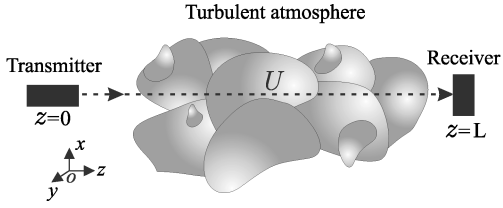

Figure 1. Geometry of optical wave propagation.

For simplicity consider only the stationary case assuming that $n(\vec{\rho}, t)$ depends only on the spatial variable $\vec{\rho}$. This assumption corresponds to the so-called 'frozen' turbulence model. Further assume that turbulent fluctuations are *locally homogeneous* and *isotropic*. In this case the statistical properties of the random function $n(\vec{\rho})$ can be described by the structure function $D_n(\rho) = \langle [n(\vec{\rho}_1) - n(\vec{\rho}_2)]^2 \rangle$, where $\vec{\rho}_1$ and $\vec{\rho}_2$ are vectors, and $\rho = |\vec{\rho}_1 - \vec{\rho}_2|$. The structure function of locally homogeneous isotropic turbulence was found by Kolmogorov and Obukhov [15, 16]. It was shown that when ρ belongs to the so-called *inertial subrange*, the structure function satisfies the following 'two thirds' law [14]

$$D_n(\rho) = C_n^2 \rho^{\frac{2}{3}}, \; l_0 < \rho \ll L_0,$$

where C_n^2 is the *structure parameter*, and l_0 and L_0 are the turbulence *inner* and *outer scales*, respectively.

The structure parameter C_n^2 depends on many factors: the propagation geometry, geographical location, the time of the year and day, and atmospheric conditions [17, 18]. The inner scale l_0 corresponds to the smallest size of inhomogeneities and is typically on the order of 1–10 mm. The outer scale L_0 defines the distances for which correlations between refractive index fluctuations still exist. The outer scale L_0 varies from hundreds of metres to several kilometres.

The Kolmogorov power-spectrum function (Fourier transform of the structure function) is given by

$$\Phi(\varkappa) = \Phi_n(\varkappa) = 0.033\, C_n^2 \varkappa^{-\frac{11}{3}}, \tag{2}$$

where $\varkappa = |\vec{\varkappa}|$, $\vec{\varkappa} = (\lambda, \mu, \nu)$ is a vector of spectral variables. For convenience of analysis and to maintain the continuity of the spectrum function for all $\varkappa$, the von Karman model is commonly used [19]

$$\Phi(\varkappa) = 0.033\, C_n^2 (\varkappa^2 + \beta^2)^{-\frac{11}{6}} e^{-\frac{\varkappa^2}{\alpha^2}}. \tag{3}$$

This model directly includes the inner and outer scales. Here $\alpha = 5.92/l_0$ and $\beta = 2\pi/L_0$. In many applications the ratio l_0/L_0 is rather small (less than 0.001), so instead of von Karman's spectrum, the Tatarskii power spectrum model

$$\Phi(\varkappa) = 0.033\, C_n^2 (\varkappa^2 + \beta^2)^{-\frac{11}{6}} \tag{4}$$

is frequently used (see Section 4.2 below). As shown below, the power spectrum models (2)–(4) are directly used for the generation of random function realizations n [20, 21].

In the framework of the layered phase distorting medium model the impact of refractive index fluctuations on wave propagation over distance $[0, L]$ is accounted for only in the discrete set of planes $\{(x, y, z) \,|\, z = z_m\}$, where $\{z_m\}_{m=0}^{M} \in [0, L]$ and $z_0 = 0, z_M = L$. In this model wave propagation through a thin phase screen at $z = z_m$ results in the corresponding random deviation (fluctuation) $S_m(\vec{r})$ of the propagating wave phase [22]. To obtain an accurate approximation of the propagation equation (1) the intervals (z_{m-1}, z_m) should be small. At the same time the distances $z_m - z_{m-1} > 0$ should exceed the refractive index fluctuation correlation length along the wave propagation direction (Oz-direction).

The correlation function of phase fluctuation $B_{S_m}(\vec{r}, z_m) = \langle S_m(\vec{r}_0) S_m(\vec{r}_0 + \vec{r}) \rangle$ and the power spectrum $\Phi(\varkappa)$ are linked by the following relationship [14]

$$B_{S_m}(\vec{r}, z_m) = 2\pi k^2 (z_m - z_{m-1}) \int\limits_{\mathbb{R}^2} e^{i(\vec{\kappa}, \vec{r})} \Phi(\kappa) d^2\vec{\kappa}, \; m \in \{1, \ldots, M\}, \tag{5}$$

where $\vec{\kappa} = (\lambda, \mu)$, $\kappa = |\vec{\kappa}|$, and $d^2\vec{\kappa} = d\lambda d\mu$. Here $(\vec{\kappa}, \vec{r})$ defines the scalar product of vectors $\vec{\kappa}$ and $\vec{r}$. Thus the problem of phase screen generation is reduced to simulation of a set of random functions $S_m(\vec{r})$ which obey (5). The random functions $S_m(\vec{r})$ are referred to as phase screens.

3. Phase screen generation in a bounded region

3.1 *Phase screen generation in a square*

For further analysis it is convenient to use a more general case of a *complex* random function $S_m(\vec{r})$ and represent this function in terms of the so-called *stochastic* integral as [22, 23]

$$S_m(\vec{r}) = S(\vec{r}; z_m) = A_m \int\limits_{\mathbb{R}^2} e^{i(\vec{\kappa},\vec{r})} Z_m(d^2\vec{\kappa}). \tag{6}$$

Here $A_m = k\sqrt{2\pi(z_m - z_{m-1})}$, and $Z_m(d^2\vec{\kappa})$ is a centered complex random measure in $\mathbb{R}^2$ with orthogonal values. It means that

$$\langle Z_m(d^2\vec{\kappa})\overline{Z_m(d^2\vec{\kappa}')}\rangle = \underline{\delta}(\vec{\kappa} - \vec{\kappa}')\Phi(\kappa)d^2\vec{\kappa}d^2\vec{\kappa}'$$

where $\underline{\delta}(\vec{\kappa})$ is the Dirac delta function, and $\overline{Z_m(d^2\vec{\kappa}')}$ is the complex conjugate to $Z_m(d^2\vec{\kappa}')$. Since the functions $S_m(\vec{r})$ are independent, we can omit the index m in all further notation. In order to simplify notation we consider equidistantly located phase screens only, so that $A_m = A$ for all m.

As a rule, in numerical simulations the stochastic integral (6) is represented in a square region $Q = [-q, q]_x \times [-q, q]_y \subset \mathbb{R}^2$ with side length $2q$ and centered at the origin. As discussed in Section 1, it is often desired to generate phase screens in non-square domains, such as rectangles $P = [-p, p]_x \times [-q, q]_y$, $p > q$. In principle it is always possible to find a rectangular region inside a square $Q_1 \supset P$, but clearly this method of phase screen modeling in rectangles is quite ineffective for $p \gg q$. Moreover, for simulating random phase screens in unbounded domains like a half-band $K = [0, +\infty)_x \times [-q, q]_y$, the above-mentioned methods cannot be applied.

Prior to describing the methods of phase screen generation in a rectangle and half-band, consider first the conventionally used approach for random function $S(\vec{r})$ generation in a square.

Define $\vec{r} = (x, y) \in Q = [-q, q]_x \times [-q, q]_y \subset \mathbb{R}^2_{\vec{r}}$ as spatial and $\vec{\kappa} = (\lambda, \mu) \in \mathbb{R}^2_{\vec{\kappa}}$ as spectral coordinates and assume that outside some square region $\Omega = [-\omega, \omega]_\lambda \times [-\omega, \omega]_\mu \subset \mathbb{R}^2_{\vec{\kappa}}$ the power spectrum Φ is negligibly small. For a fixed $\vec{r}$ the stochastic integral (6) represents the mean-square limit of its integral sums (see, for example, [24]). Let $\delta > 0$ be the step in the spectral domain Ω, $(\lambda_k, \mu_l) = (k\delta, l\delta)$ for $k, l \in \{-N, \dots, N\}$, where $N = \omega/\delta$ is some positive integer associated with the numerical grid points in the spectral domain (see figure 2).

For $(x, y) \in Q$ the approximation of S using the grid points in the spectral domain (denoted by $\tilde{S}$) can be represented as the following sum

$$\tilde{S}(x, y) = A \sum_{k=-N}^{N-1} \sum_{l=-N}^{N-1} e^{i(\lambda_k x + \mu_l y)} \sqrt{\Phi(\lambda_k, \mu_l)}\, \eta(d\lambda_k, d\mu_l), \tag{7}$$

where $\eta(d\lambda, d\mu)$ is a centered random measure in Ω with orthogonal values, the structural measure of which is equal to the Lebesgue measure in $\mathbb{R}^2$, $(d\lambda_k, d\mu_l) = [\lambda_k, \lambda_{k+1}] \times [\mu_l, \mu_{l+1}]$. In other words, for the random measure $\eta(d\lambda, d\mu)$ the following properties hold

$$\langle \eta(d\lambda_k, d\mu_l)\rangle = 0,$$
$$\langle \eta(d\lambda_k, d\mu_l)\overline{\eta(d\lambda_{k'}, d\mu_{l'})}\rangle = \underline{\delta}_{kk'}\underline{\delta}_{ll'}\delta^2,$$

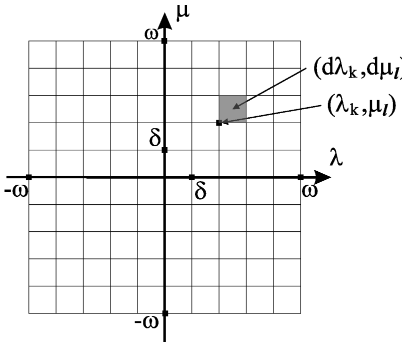

Figure 2. Partition of the spectral domain Ω for phase screen generation in a square.

where $\underline{\delta}_{kk'}$ and $\underline{\delta}_{ll'}$ are the Kronecker symbols. Consider the approximation of (7) on a discrete set of values $x, y \in Q$ corresponding to numerical grid points assuming that $\mathrm{d} = q/N$ is the distance between the adjacent grid points so that $(x_m, y_n) = (m\mathrm{d}, n\mathrm{d})$ for $m, n \in \{-N, \ldots, N-1\}$. The sum (7) is now given by

$$\tilde{S}(m\mathrm{d}, n\mathrm{d}) = A \sum_{k=-N}^{N-1} \sum_{l=-N}^{N-1} e^{i\mathrm{d}\delta(km+ln)} \sqrt{\tilde{\Phi}_{kl}} \tilde{\eta}_{kl} = AF_{(k,l)} \left\{ \sqrt{\tilde{\Phi}} \tilde{\eta} \right\} (m, n), \tag{8}$$

where $m, n \in \{-N, \ldots, N-1\}$, $\tilde{\Phi}_{kl} = \Phi(\lambda_k, \mu_l)$, $\tilde{\eta}_{kl} = \eta(d\lambda_k, d\mu_l)$, and $F_{(k,l)}$ denotes the 'discrete version' of the Fourier transform with respect to the variables (indices) k and l. Note that in the approximation (8) it is assumed that $\omega q = \pi N$ or $\delta\mathrm{d} = \pi/N$.

In the standard computer code for the discrete Fourier transform (DFT) the indices $m' = m + N$, $n' = n + N$, $k' = k + N$, $l' = l + N$ are frequently used, so that each of these new indices belongs to the set $\{0, \ldots, M-1\}$, where $M = 2N$. Then we obtain

$$\begin{aligned}\tilde{S}(m\mathrm{d}, n\mathrm{d}) &= A \sum_{k'=0}^{M-1} \sum_{l'=0}^{M-1} e^{\frac{2\pi i}{M}((k'-N)(m'-N)+(l'-N)(n'-N))} \sqrt{\tilde{\Phi}_{k'l'}^{-N}}\, \tilde{\eta}_{k'l'}^{-N} \\ &= AFT_{(k',l')} \left\{ \sqrt{\tilde{\Phi}^{-N}}\, \tilde{\eta}^{-N} \right\} (m', n'),\end{aligned} \tag{9}$$

where $\tilde{\Phi}_{k'l'}^{-N} = \tilde{\Phi}_{(k'-N)(l'-N)}$, $\tilde{\eta}_{k'l'}^{-N} = \tilde{\eta}_{(k'-N)(l'-N)}$ and the operator $FT_{(k,l)}$ denotes the digital Fourier transform [25].

Examples of random phase screen generation using equation (9) are presented in figure 3.

In these examples the random measure η in (9) is approximated using M^2 statistically independent uniformly distributed random complex numbers $\{\tilde{\eta}_{kl}\}_{k,l=-N}^{N-1}$, satisfying the following

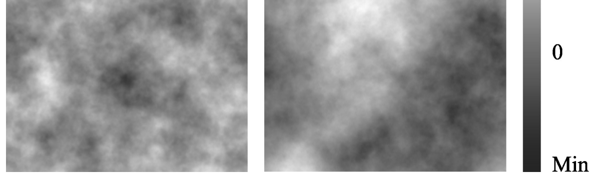

Figure 3. Examples of pseudo-random phase screens for von Karman (left) and Kolmogorov (right) power spectrum models generated on the numerical grid of size 256×256.

conditions

$$\langle \tilde{\eta}_{kl} \rangle = 0, \quad \langle |\tilde{\eta}_{kl}|^2 \rangle = \delta^2 \text{ for all } k, l \in \{-N, \ldots, N-1\}.$$

Under these conditions the second moments of the random function $\tilde{S}$ (in particular, its correlation function $\tilde{B_S}$) do not depend on a specific choice of the random number distribution $\tilde{\eta}_{kl}$.

It is easy to show that approximation of the correlation function for $\tilde{S}$ is given by the expressions

$$\tilde{B_S}(x_0, y_0, x_0 + x, y_0 + y) = \tilde{B_S}(x, y) = A^2 \delta^2 \sum_{k=-N}^{N-1} \sum_{l=-N}^{N-1} e^{i(\lambda_k x + \mu_l y)} \tilde{\Phi}_{kl}. \tag{10}$$

3.2 *Error estimates of the approximation*

To estimate the approximation error of the correlation function B_S consider as an example the Tatarskii spectrum function. Notice that for Kolmogorov's spectrum function such estimations make no sense because the corresponding integrals, in particular, the variance function $B_S(0, 0)$, are infinite. From expressions (5) and (10) it follows that

$$B_S(x, y) = A^2 \int_{\mathbb{R}^2} e^{i(\lambda x + \mu y)} \Phi(\lambda, \mu) d\lambda d\mu, \quad B_S(0, 0) = A^2 \int_{\mathbb{R}^2} \Phi(\lambda, \mu) d\lambda d\mu,$$

and

$$|B_S(x, y) - \tilde{B_S}(x, y)| \le A^2 \int_{\mathbb{R}^2 \setminus \Omega} \Phi(\lambda, \mu) d\lambda d\mu$$
$$+ A^2 \sum_{k=-N}^{N-1} \sum_{l=-N}^{N-1} \int_{(d\lambda_k, d\mu_l)} \left| e^{i(\lambda x + \mu y)} \Phi(\lambda, \mu) - e^{i(\lambda_k x + \mu_l y)} \Phi(\lambda_k, \mu_l) \right| d\lambda d\mu.$$

Since $|e^{ip} - 1| \le |p|$ for any real p, for $(\lambda, \mu) \in (d\lambda_k, d\mu_l)$ with some $(\tilde{\lambda}_k, \tilde{\mu}_l) \in (d\lambda_k, d\mu_l)$ we obtain

$$\left| e^{i(\lambda x + \mu y)} \Phi(\lambda, \mu) - e^{i(\lambda_k x + \mu_l y)} \Phi(\lambda_k, \mu_l) \right| \le |\Phi(\lambda, \mu) - \Phi(\lambda_k, \mu_l)|$$
$$+ \left| e^{i(\lambda x + \mu y)} - e^{i(\lambda_k x + \mu_l y)} \right| \Phi(\lambda, \mu) \le \sqrt{2}\delta \left| \nabla \Phi(\tilde{\lambda}_k, \tilde{\mu}_l) \right| + \delta \left(|x| + |y| \right) \Phi(\lambda, \mu).$$

Therefore the approximation error is given by

$$\left| B_S(x, y) - \tilde{B_S}(x, y) \right| \le \delta(|x| + |y|) B_S(0, 0)) + \delta \Psi_1(\delta) + \Psi_2(\omega), \tag{11}$$

where

$$\Psi_1(\delta) \to A^2 \sqrt{2} \int_{\Omega} |\nabla \Phi(\lambda, \mu)| d\lambda d\mu \le A^2 \sqrt{2} \int_{\mathbb{R}^2} |\nabla \Phi(\lambda, \mu)| d\lambda d\mu,$$

for $\delta \to 0$, and

$$\Psi_2(\omega) \le A^2 \int_{\mathbb{R}^2 \setminus \Omega} \Phi(\lambda, \mu) d\lambda d\mu \to 0$$

for $\omega \to +\infty$. Thus, in order to obtain the desired accuracy for bigger values of $|x|$ (but the same $|y|$), it suffices to take proportionally smaller steps in δ in the Ox-direction. It is easily seen that the functions $\tilde{S}(x, y)$ and $\tilde{B_S}(x, y)$ are $2q$-periodic with respect to the variables x and y.

3.3 *Phase screen generation in a rectangle*

Consider now phase screen generation in a rectangle $P = [-p, p]_x \times [-q, q]_y$, where $p = Rq$ and $R > 1$ is an integer. Our goal is to modify formulas (7), (8) and (9) by keeping the accuracy of the corresponding approximation for B_S in rectangles unchanged. Subdivide each interval $[\lambda_k, \lambda_{k+1}]$, $k \in \{-N, \ldots, N-1\}$ using the additional grid points $\{\lambda_{k+\frac{j}{R}}\} = \{(k + j/R)\delta\}$, $j \in \{0, \ldots R-1\}$ (see figure 4).

The total number of grid points resulting from such partitioning of $[-\omega, \omega]$ is equal to $2NR$. By analogy with (7) we can write

$$\tilde{S}(x, y) = \sum_{k=-N}^{N-1} \sum_{j=0}^{R-1} \sum_{l=-N}^{N-1} e^{i(\lambda_{k+j/R}x + \mu_l y)} \sqrt{\Phi(\lambda_{k+j/R}, \mu_l)}\, \eta(d\lambda_{k+j/R}, d\mu_l), \tag{12}$$

where $(d\lambda_{k+j/R}, d\mu_l) = [\lambda_{k+j/R}, \lambda_{k+(j+1)/R}] \times [\mu_l, \mu_{l+1}]$. Approximating each $\Phi(\lambda_{k+j/R}, \mu_l)$ by $\Phi(\lambda_k, \mu_l) = \tilde{\Phi}_{kl}$, we can simplify (with some small error) the sum (12) as follows

$$\tilde{S}(x, y) = \sum_{k=-N}^{N-1} \sum_{l=-N}^{N-1} \sqrt{\tilde{\Phi}_{kl}}\, e^{i(\lambda_k x + \mu_l y)} \left(\sum_{j=0}^{R-1} e^{i\delta x j/R} \eta(d\lambda_{k+j/R}, d\mu_l) \right), \tag{13}$$

for $(x, y) \in P$. By analogy, for the discrete version we obtain

$$\begin{aligned} \tilde{S}(m\mathrm{d}, n\mathrm{d}) &= \sum_{k=-N}^{N-1} \sum_{l=-N}^{N-1} \sqrt{\tilde{\Phi}_{kl}}\, e^{i\mathrm{d}\delta(km+ln)} \left(\sum_{j=0}^{R-1} e^{i\mathrm{d}\delta m j/R} \tilde{\eta}_{(k+j/R)l} \right) \\ &= \sum_{j=0}^{R-1} e^{i\mathrm{d}\delta m j/R} F_{(k,l)} \left\{ \sqrt{\tilde{\Phi}} \tilde{\eta}^j \right\}(m, n), \end{aligned} \tag{14}$$

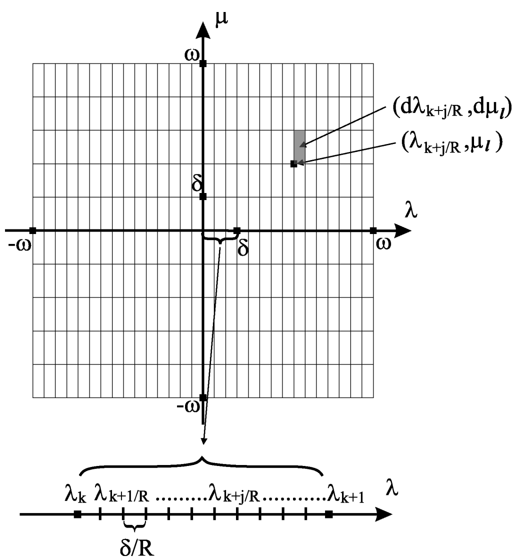

Figure 4. Partition of the spectral domain for modeling random phase screens in the rectangle P.

where $m \in \{-RN, \ldots, RN-1\}$, $n \in \{-N, \ldots, N-1\}$, and we set $\tilde{\eta}^j_{kl} = \eta(d\lambda_{k+j/R}, d\mu_l)$. It is straightforward to obtain the corresponding 'standard' (analogous to (9)) DFT version of the last formula. From the expression (14) it is clear that the required computational time for phase screen generation in the rectangle grows proportionally to R.

The generation of 'long' pseudo-random phase screens in a rectangle using formula (14) can be performed in several steps. The first step includes generation of R independent screens $\tilde{S}^j(m\mathrm{d}, n\mathrm{d})$ on the square grid $M \times M$ (see Section 3.1). These phase screens are assumed to be M-periodic with respect to index m. At the second step the generated phase screens $\tilde{S}^j$ are multiplied by the exponential factors $e^{(i\mathrm{d}\delta mj/R)}$ defined on the numerical grid $RM \times M$. The final step includes summation of the R components $\tilde{S}^j(m\mathrm{d}, n\mathrm{d})e^{(i\mathrm{d}\delta mj/R)}$. An example of phase screen generation in a rectangle region using (14) is shown in figure 5.

Since $\tilde{\eta}^j_{kl}$ satisfies the property

$$\left\langle \tilde{\eta}^j_{kl}\overline{\tilde{\eta}^{j'}_{k'l'}} \right\rangle = \underline{\delta}_{kk'}\underline{\delta}_{ll'}\underline{\delta}_{jj'}\delta^2/R,$$

the correlation function corresponding to (14) has the form

$$\tilde{B_S}(x, y) = (\delta^2/R) \sum_{k=-N}^{N-1} \sum_{l=-N}^{N-1} \tilde{\Phi}_{kl} e^{i(\lambda_k x + \mu_l y)} \left(\sum_{j=0}^{R-1} e^{i\delta xj/R} \right)$$

or in the discrete case,

$$\tilde{B_S}(m\mathrm{d}, n\mathrm{d}) = (\delta^2/R) \left(\sum_{j=0}^{R-1} e^{i\mathrm{d}\delta mj/R} \right) F_{(k,l)}\{\tilde{\Phi}\}(m, n).$$

The corresponding error estimates for B_S in a rectangle are almost the same as in (11), in spite of the fact that we have used $\Phi(\lambda_k, \mu_l)$ instead of $\Phi(\lambda_{k+\frac{j}{R}}, \mu_l)$ in (12) for all $j \in \{0, \ldots R-1\}$. Note that the functions $\tilde{S}(x, y)$ and $\tilde{B_S}(x, y)$ are $2Rq$-periodic with respect to the variable x and $2q$-periodic with respect to y.

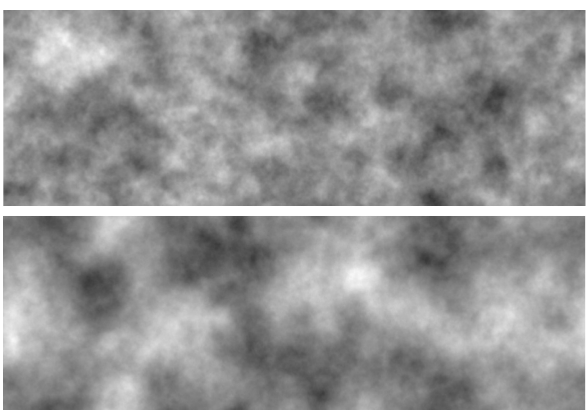

Figure 5. Pseudo-random phase screens generated in a rectangular region with $M = 256$ and $R = 3$ for the von Karman (top) and Kolmogorov (bottom) power spectrum models.

3.4 *Phase screens generation with large-scale inhomogeneities based on spectral-band partitioning method*

As mentioned in Section 2 Kolmogorov's 'two thirds' law takes place only inside the inertial interval defined by the inner l_0 and outer L_0 scales that define the range of the characteristic scales of optical inhomogeneities in atmospheric turbulence. In realistic conditions the ratio L_0/l_0 can be as big as 10^4–10^6 [22, 27, 28]. This poses a serious problem for adequate representation of phase screens on a numerical grid where the smallest scale of inhomogeneities is associated with the distance between grid points, and the largest scale is typically described by the grid size M. Thus in numerical simulations the ratio of the largest to the smallest scales doesn't exceed M which is significantly smaller than L_0/l_0. In this section we describe the mathematical technique for generation of phase screens with the extended (long-range) phase non-homogeneities of size (correlation length) exceeding the transverse (in the Oy-direction) size of the numerical simulation domain (domains Q or P). Note that, as mentioned in Section 3.3, the generated phase screens $\tilde{S}(x, y)$ are $2Rq$-periodic with respect to x and $2q$-periodic with respect to y.

Consider the method for generation of turbulent screens with large-scale phase inhomogeneities ('long-range correlations'). Let $R = 2_H$ where H is a natural number. Define the spatial domains $P_h = [-p, p]_x \times [-2^{H-h}q, 2^{H-h}q]_y$, where $h \in \{0, \ldots, H\}$ (thus $P_0 \supset P_1 \supset \cdots \supset P_H$), and consider partitioning of the spectral plane $\mathbb{R}^2_{\vec{\kappa}}$ into annuluses $\{\kappa < r_1\}$, $\{r_1 \leqslant \kappa < r_2\}$, $\{r_2 \leqslant \kappa < r_3\}, \ldots,$ $\{r_H \leqslant \kappa\}$ (all together $H + 1$ annuluses). For $h \in \{0, \ldots, H\}$ consider the functions

$$\Phi_h(\kappa) = \begin{cases} \Phi(\kappa) & \text{for } \vec{\kappa} \in \{r_h \leqslant \kappa < r_{h+1}\}; \\ 0 & \text{for } \vec{\kappa} \notin \{r_h \leqslant \kappa < r_{h+1}\}, \end{cases}$$

where we set $r_0 = 0$, $r_{H+1} = +\infty$. Assume $\Phi = \sum_{h=0}^{H} \Phi_h$ and define the random function S by the expression

$$S(\vec{r}) = \sum_{h=0}^{H} \int_{\mathbb{R}^2} e^{i(\vec{\kappa},\vec{r})} Z_h(d^2\vec{\kappa}) = \sum_{h=0}^{H} S_h(\vec{r}), \tag{15}$$

where $\langle Z_h(d^2\vec{\kappa})\overline{Z_{h'}(d^2\vec{\kappa}')}\rangle = \underline{\delta}_{hh'}\underline{\delta}(\vec{\kappa}-\vec{\kappa}')\Phi_h(\kappa)d^2\vec{\kappa}d^2\vec{\kappa}'$. Clearly, each random function component S_h corresponds to spatial filtering of S using a band-pass filter. The generation of S_h can be performed in the domain P_h using the method described in Section 3.3.

Assume that for all h the grid size M is identical and consider discrete approximations $\tilde{S}_h$ of the random components $S_h(\vec{r})$ in (15). These components are defined on the grid $(2^h M)\times(M)$. Since all domains P_H have the same size in the Ox-direction, the discrete approximation $\tilde{S}$ of the function S represents the sum of the functions $\tilde{S}_h$ defined on the extended grid $(2^H M)\times(M)$. The calculations of the random components $\tilde{S}_h$ can be obtained using various interpolation methods (e.g. the B-splines technique). Note that for small enough h this interpolation doesn't lead to any practical loss of accuracy in the approximation because for small h the spectrum function of $\tilde{S}_h$ contains only the low-frequency components so that $\tilde{S}_h$ is a slowly changing function. It is easy to see that the step in the spectral domain depends on h; it is equal to $\delta_h = 2\pi/(2^{(H-h+1)}q)$. Therefore, the low-frequency region of the spatial spectrum is now approximated with better accuracy than in the previously discussed methods. The spectral-band partitioning method can be used for generation of pseudo-random phase screens with large-scale phase non-homogeneities. The method is illustrated in figure 6.

Notice that there is some freedom in the spectral band partitioning (choice of the sequence $\{r_h\}_{h=1}^{H}$) that can be used for obtaining optimal models for different wave propagation

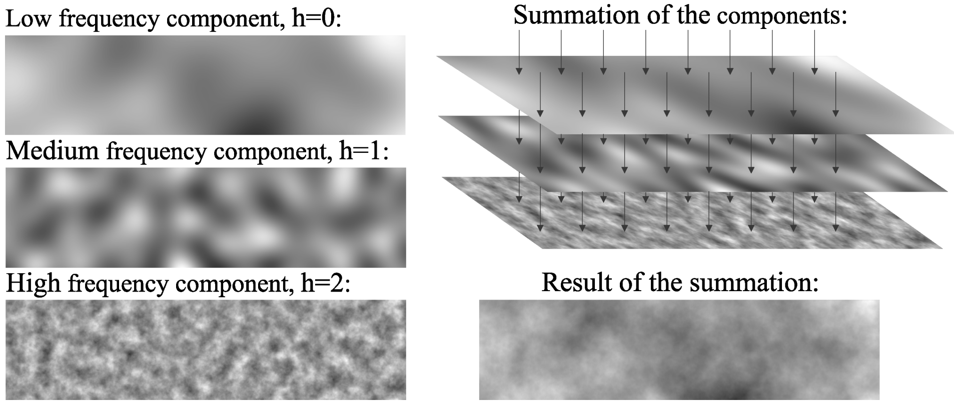

Figure 6. Schematic of phase screen generation using spectral-band partitioning method. The grey-scale images at right correspond to the random function components $\tilde{S}_h$, where $h = 0$ for the upper image, $h = 1$ for the middle image and $h = 2$ for the bottom image. These images are obtained using the spline interpolation scheme. The phase screen with large-scale inhomogeneities (bottom image at the right) is obtained by summation of the components $\tilde{S}_h$ as illustrated by the top images at the right. The phase screen $\tilde{S}$ corresponds to the Kolmogorov turbulence model with $M = 256$, $R = 4$ $(H = 2)$.

scenarios. The screens obtained by this method are $2^H M = RM$-periodic with respect to the variables m and n. Finally, notice that this method can be easily generalized for the case $R = \alpha_1 2^{H_2}$, where H_1, H_2 are natural numbers.

4. Phase screen generation in a half-band

4.1 *'Infinite' phase screen generation via the splicing function method*

Consider phase screen generation in a half-band $K = [0, +\infty)_x \times [-q, q]_y$. Take a sequence of random functions $\{S_j\}_{j=0}^{+\infty}$ defined as

$$S_j(\vec{r}) = A \int\limits_{\mathbb{R}^2} e^{i(\vec{\kappa},\vec{r})}\, Z_j(d^2\vec{\kappa}),$$

where, similarly to (6), $A_m = A$, and Z_j are the mutually independent random measures corresponding to the power spectrum Φ dependent on the parameters C_n^2, l_0 and L_0. The functions S_j are considered statistically mutually independent with (the same) correlation functions $B_S(x, y)$ (see (5) and (23), (26) below).

Set $p = Rq$ ($R > 1$ is a natural number) and consider a family of real-valued non-negative functions $\{\psi_j\}_{j=0}^{+\infty}$ continuous inside $\mathbb{R}$ (splicing functions) such that the support of ψ_j belongs to $[(j-1)p, (j+1)p]$ for each j, that is, $\psi_j = 0$ outside $[(j-1)p, (j+1)p]$. Define the function, referred to as an 'infinite' phase screen, as

$$S_\infty(x, y) = \sum_{j=0}^{+\infty} \psi_j(x) S_j(x - jp, y). \tag{16}$$

Clearly, the series (16) on each compact set of points (x, y) in K is a finite sum, so that S_∞ is an L_2-process. From the continuity of B_S and ψ_j for each j it follows that S_∞ is the mean square continuous L_2-process (see [24]) that can be considered as an 'unbounded' (infinite) random function. Calculate the correlation function of S_∞ using the mutual statistical independence of S_j

$$B_{S_\infty}(x_0, y_0, x_0 + x, y_0 + y) = B_S(x, y) \sum_{j=0}^{+\infty} \psi_j(x_0)\psi_j(x_0 + x). \tag{17}$$

The *splicing* functions ψ_j are in our hands, and it is reasonable to choose them in such a way that the function B_{S_∞} would approximate B_S as well as possible for $(x_0, y_0) \in K$ and $|y| < q$, $0 < x < L_0$. On the other hand, ψ_j should have a more or less simple form. In this respect we consider the following two requirements on $\{\psi_j\}$. First, we require that $B_{S_\infty}(x_0, y_0, x_0, y_0) = B_S(0, 0)$, which means that the variance of both S and S_∞ random functions coincides for all points $(x_0, y_0) \in K$. From this condition it follows that

$$\sum_{j=0}^{+\infty} [\psi_j(x_0)]^2 \equiv 1 \tag{18}$$

for all $x_0 \in [0, +\infty)$. Therefore, for each $j \geq 0$ one can find a continuous function f_j : $[jp, (j+1)p] \to [0, \pi/2]$ such that $f_j(jp) = 0$, $f_j[(j+1)p] = \pi/2$ and $\psi_j(\tau) = \cos(f_j(\tau))$, $\psi_{j+1}(\tau) = \sin(f_j(\tau))$ for all $\tau \in [jp, (j+1)p]$. Second, for simplicity, we choose the functions f_j to be linear (on $[jp, (j + 1)p]$). In this case for the family of functions

$$\psi_0(\tau) = \begin{cases} \cos(\frac{\pi\tau}{2p}) & \text{for } \tau \in [-p, p]; \\ 0 & \text{for } \tau \notin [-p, p] \end{cases} \tag{19}$$

and

$$\psi_j(\tau) = \psi_0(\tau - jp), \quad j = 1, 2, \ldots, \tag{20}$$

the requirement (18) is satisfied. For the chosen $\{\psi_j\}$, elementary calculations show that for all $x_0 \geq 0$ and $x \geq 0$ the following inequality holds:

$$|B_S(x, y) - B_{S_\infty}(x_0, y_0, x_0 + x, y_0 + y)| \leq |B_S(x, y)| \frac{\pi^2 x^2}{8p^2}. \tag{21}$$

Since by (17), (19) and (20) we always have $|B_S(x, y) - B_{S_\infty}(x_0, y_0, x_0 + x, y_0 + y)| \leq |B_S(x, y)|$, the inequality (21) makes sense only for $0 \leq x \leq p$. Moreover, as it is shown in the following section, $B_S(x, y)/B_S(0, 0) < 0.0043$ (is 'almost zero') for $x \geq L_0$, so that the estimate (21) will be considered only for $x \leq L_0$.

In applications (on each appropriate interval of time), in fact, we use only a portion of the screen with a length much smaller than L_0. So the following notations and estimates seem useful. Given $\sigma \in (0, 1)$ and $\varepsilon \in (0, 1)$, we say that the estimate B_{S_∞} of B_S is (σ, ε)-*precise* (uniformly for $x_0 \geq 0$), if the inequality

$$|B_{S_\infty}(x_0, y_0, x_0 + x, y_0 + y) - B_S(x, y)| \leqslant \varepsilon\, |B_S(x, y)| \tag{22}$$

holds for all $x_0 \geq 0$ and $0 \leq x \leq \sigma L_0$.

From (21) it follows that, in order to have a (σ, ε)-precise estimate, we have to take $p \geq \pi\sigma L_0/\sqrt{8\varepsilon}$. Roughly speaking, in order to generate a (σ, ε)-precise 'very long' screen S_∞ on $[0, X_0]_x \times [-q, q]_y$, it is enough to generate a sequence of $(\sigma, \varepsilon/3)$-precise phase screens S_j on $[-p, p]_x \times [-q, q]_y$ for $j = 0, 1, \cdots, [X_0/p]$ with $p = \pi\sigma L_0/\sqrt{8\varepsilon}$.

Consider the generation of infinite phase screens on *numerical grid*. Assume $\{\tilde{S}_j(m\mathrm{d}, n\mathrm{d})\}_{j=0}^{+\infty}$ is a family of independent random phase screens defined on the grid $2RN \times 2N$ (see Section 3.4), that is $m \in \{-RN, \ldots, RN - 1\}$, $n \in \{-N, \ldots, N - 1\}$. In fact $\tilde{S}_j(m\mathrm{d}, n\mathrm{d})$ (just by its formula (14)) is considered as $2RN$-periodic with respect to m.

Set, by (16),

$$\tilde{S}_\infty(m\mathrm{d}, n\mathrm{d}) = \sum_{j=0}^{+\infty} \psi_j(m\mathrm{d})\tilde{S}_j(m\mathrm{d} - RNj\mathrm{d}, n\mathrm{d}),$$

where $m \geq 0$, $n \in \{-N, \ldots, N-1\}$.

The procedure for the infinite phase screen generation is schematically illustrated in figure 7.

It includes the following steps:

- Generation of the initial phase screen $\tilde{S}_0(m\mathrm{d}, n\mathrm{d})$ of length RN (we need only the 'right-hand side' of the screen, defined on $\tilde{P}_0 = \{0, \ldots, RN-1\}_m \times \{-N, \ldots, N-1\}_n$).
- On step $j \geq 0$. Generation of a statistically independent (of all the previous screens $\tilde{S}_{j'}$) phase screen $\tilde{S}_{j+1}(m\mathrm{d}, n\mathrm{d})$ of length $2RN$. Splicing the (right-hand side of the) screen $\tilde{S}_j$ with the (left-hand side of the) screen $\tilde{S}_{j+1}$ on the set $\tilde{P}_j = \{RNj, \ldots, RN(j+1)-1\}_m \times \{-N, \ldots, N-1\}_n$ by (pointwise) multiplying $\tilde{S}_j(m\mathrm{d} - RNj\mathrm{d}, n\mathrm{d})$ by $\cos(\pi(m - RNj)/2RN)$ and $\tilde{S}_{j+1}(m\mathrm{d} - RN(j+1)\mathrm{d}, n\mathrm{d})$ by $\sin(\pi(m - RNj)/2RN)$ and summing. As a result we obtain the values of $\tilde{S}_\infty$ on $\tilde{P}_j$.

This algorithm provides an effective (in the sense of computational time) method to simulate pseudo-random phase screens $\tilde{S}_\infty$ of any required length.

4.2 *'Infinite' phase screens with slowly varying statistical characteristics*

It is well known that the atmospheric turbulence parameters such as structural constant C_n^2 and the inner l_0 and outer L_0 scales are functions of altitude above the ground [17, 18, 26]. As a result, in the propagation scenarios with altitude change for either a light source

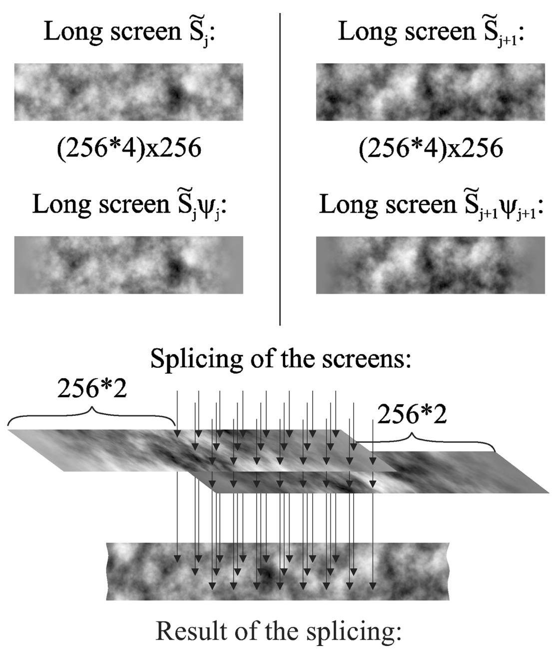

Figure 7. One step of the algorithm for the infinitely extended phase screen generation using Von Karman's model of the spectrum. $M = 256$, $R = 4$.

or an optical receiver or both such as laser tracking of low-altitude targets, airborne wide angular range optical sensing and imaging, these atmospheric turbulence parameters can no longer be considered as constant values. In numerical analysis these changes in the major atmospheric characteristics can be accounted for by generating phase screens with slowly varying turbulence parameters along a predefined spatial direction related to the light source or optical receiver altitude change. Here we consider infinite phase screen generation with slow-varying statistical characteristics along the coordinate x direction only.

Before going on, we have to obtain some convenient representations (similar to that of [22], p. 49) for the correlation function B_S, given by (5) (here the parameters C_n^2, l_0 and L_0 are still constant)

$$B_S(\vec{r}) = A^2 \int_{\mathbb{R}^2} e^{i(\vec{\kappa},\vec{r})}\Phi(\kappa)d^2\vec{\kappa} = B_S(r) = 2\pi A^2 \int_0^{+\infty} \Phi(\kappa)J_0(r\kappa)\kappa d\kappa, \tag{23}$$

where $r = |\vec{r}|$ and J_0 is a Bessel function of the first kind and order zero. Assume that $\Phi(\kappa)$ in (23) is the von Karman power spectrum function (3). After changing variables $u = \kappa/\beta$ we obtain

$$B_S(r) = 3C^2\beta^{-5/3}F_\alpha^\beta(r)/5, \tag{24}$$

where

$$F_\alpha^\beta(r) = \frac{5}{3}\int_0^{+\infty} \frac{e^{-\left(\frac{\beta}{\alpha}\right)^2 u^2} J_0(\beta r u)udu}{(u^2+1)^{\frac{11}{6}}}, \tag{25}$$

and $C = A\sqrt{0.066\pi}C_n$. Since $\beta/\alpha = 2\pi l_0/(5.92L_0)$ is typically smaller than 0.001, the integral in (25) can be well-approximated by the value $F(\beta r)$ of the following simpler integral

$$F(p) = \frac{5}{3}\int_0^{+\infty} \frac{J_0(pu)udu}{(u^2+1)^{\frac{11}{6}}}, \quad p \geq 0.$$

The last integral can be represented in the form (see [29], ch. 13, s. 6)

$$\begin{aligned} F(p) &= \Gamma\left(\frac{1}{6}\right)\sum_{k=0}^{+\infty}\frac{\left(\frac{p}{2}\right)^{2k}}{k!\Gamma\left(k+\frac{1}{6}\right)} - \frac{5\pi}{3\,\Gamma\left(\frac{11}{6}\right)2^{\frac{5}{3}}}\sum_{k=0}^{+\infty}\frac{p^{\frac{5}{3}}\left(\frac{p}{2}\right)^{2k}}{k!\Gamma\left(k+\frac{11}{6}\right)} \\ &= 1 - 1.864p^{\frac{5}{3}} + 1.5p^2 - 0.254p^{\frac{11}{3}} + \cdots. \end{aligned}$$

The function $F(p)$ also has the following asymptotic formula as $p \to +\infty$

$$F(p) \simeq F_\infty p^{\frac{1}{3}} e^{-p}\left[1 + \frac{2}{9p} + \cdots\right],$$

where $F_\infty = 5\sqrt{\pi}/\left(3\,\Gamma\left(\frac{11}{6}\right)2^{\frac{4}{3}}\right) \approx 1.250$.

Consider several useful properties of the function F. The last expressions and numerical analysis of F show that $F(p)$ is decreasing on $[0, +\infty)$, $F(0) = 1$ and for $p = \beta r \geq 2\pi$ we have $0 < F(p) < 0.0043$. The other fact (very useful for obtaining the main estimate (36) below) is that $-F'(p) < F(p),\ p > 0$. One can also prove that

$$\left|F_\alpha^\beta(r) - F(\beta r)\right| \leq \begin{cases} 6\left(\frac{\beta}{\alpha}\right)^{\frac{5}{3}} & \text{for all } r > 0\,; \\ 7.5\left(\frac{\beta}{\alpha}\right)^2 & \text{for } \beta r \geq \pi/2. \end{cases}$$

Thus, for $r \le L_0$ we also have $|F_\alpha^\beta(r) - F(\beta r)|/F(\beta r) \le 0.002$). By taking into account the obtained approximations for F_α^β and F, the correlation function (24) can be represented in the form

$$B_S(r) = \frac{3}{5} C^2 \left(\frac{L_0}{2\pi}\right)^{\frac{5}{3}} F(\beta r). \tag{26}$$

In particular, we see that $B_S(r) < 0.0043\, B_S(0)$ is (relatively) negligible for $r \ge L_0$.

Notice that formula (26) (being approximate for the von Karman spectrum function) in fact is *precise* for the Tatarskii spectrum function (4) (which corresponds to the case $\alpha = +\infty$, that is $l_0 = 0$).

Using the representation of the correlation function (26) as a basis, continue the consideration of the original problem statement of phase screen generation whose statistical characteristics $C_n^2 = C_n^2(x_0)$, $l_0 = l(x_0)$ and $L_0 = L(x_0)$ are slowly dependent on the parameter x_0. In other words, we assume that the correlation function $\langle S(x_0, y_0)\overline{S(x_0 + x, y_0 + y)}\rangle = B_S(x_0, y_0, x_0 + x, y_0 + y)$ of such phase screen S has the form

$$B_S(x_0, y_0, x_0 + x, y_0 + y) = \frac{3}{5} C^2(x_0) \left(\frac{L(x_0)}{2\pi}\right)^{\frac{5}{3}} F\left(\frac{2\pi r}{L(x_0)}\right). \tag{27}$$

For the variance function $\chi(x_0) = B_S(x_0, y_0, x_0, y_0)$ at the point (x_0, y_0) from (27) we obtain

$$\chi(x_0) = \frac{3}{5} C^2(x_0) \left(\frac{L(x_0)}{2\pi}\right)^{\frac{5}{3}}. \tag{28}$$

Notice that the method considered cannot be applied for the Kolmogorov spectrum function (2), because for this case we have $\chi(x_0) \equiv +\infty$.

Introduce a sequence $\{t_j\}_{j=0}^{+\infty}$ and the intervals $I_j = [t_j, t_{j+1}]$, where $t_0 = 0$, $\Delta_j = t_{j+1} - t_j = \theta_j L(t_j)$, and $\theta_j > 0$ are parameters (to be chosen later subsequently by induction). Consider the following sequence of functions $\{\psi_j\}_{j=1}^{+\infty}$

$$\psi_j(\tau) = \begin{cases} a_{j-1}(\tau) \cos \frac{\pi(\tau - t_j)}{2\Delta_{j-1}} & \text{for } \tau \in I_{j-1}; \\ a_j(\tau) \cos \frac{\pi(\tau - t_j)}{2\Delta_j} & \text{for } \tau \in I_j; \\ 0 & \text{for } \tau \notin (I_{j-1} \cup I_j). \end{cases} \tag{29}$$

For the case $j = 0$ set $\psi_0(\tau) = 0$ outside I_0, and define $\psi_0(\tau)$ on I_0 by the second equality in (29). The family of functions $\{a_j\}_{j=0}^{+\infty}$ is defined below.

Similarly as in Section 4.1, consider a sequence of mutually independent screens $\{S_j\}$ having von Karman's (respectively, Tatarskii's) spectrum functions with (constant) parameters $C^2(t_j)$, $l(t_j)$, respectively, $l(t_j) = 0$, and $L(t_j)$, $(j = 0, 1, \ldots)$. Define

$$S_\infty(x, y) = \sum_{j=0}^{+\infty} \psi_j(x) S_j(x - t_j, y). \tag{30}$$

The correlation function of S_∞ is given by the expression

$$B_{S_\infty}(x_0, y_0, x_0 + x, y_0 + y) = \sum_{j=0}^{+\infty} B_{S_j}(x, y)\, \psi_j(x_0)\psi_j(x_0 + x).$$

From (27) we obtain

$$B_{S_\infty}(x_0, y_0, x_0 + x, y_0 + y) = \sum_{j=0}^{+\infty} \chi(t_j)\, F\left(\frac{2\pi r}{L(t_j)}\right) \psi_j(x_0)\psi_j(x_0 + x). \tag{31}$$

Assume that the variances of random functions S and S_∞ coincide for all points $(x_0, y_0) \in K$, that is $B_{S_\infty}(x_0, y_0, x_0, y_0) = \chi(x_0)$. This assumption leads to the following condition

$$\sum_{j=0}^{+\infty} \chi(t_j)\, \psi_j^2(x_0) \equiv \chi(x_0). \tag{32}$$

This expression defines the functions $a_j(\tau)$

$$a_j(\tau) = \left[\frac{2\chi(\tau)}{\chi(t_j) + \chi(t_{j+1}) + (\chi(t_j) - \chi(t_{j+1})) \cos \frac{\pi(\tau - t_j)}{\Delta_j}} \right]^{\frac{1}{2}}. \tag{33}$$

Let us estimate the accuracy of the proposed infinite phase screen generation method in the sense of the approximation of B_S by analogy with (21). For $x_0 \geq 0$ define

$$\lambda(x_0) = \sup_{\tau \geq x_0} |L'(\tau)|, \quad \zeta(x_0) = \sup_{\tau \geq x_0} \frac{|C'(\tau)| L(\tau)}{C(\tau)}, \quad \mu(x_0) = \sup_{\tau \geq x_0} \frac{|\chi'(\tau)| L(\tau)}{\chi(\tau)}. \tag{34}$$

It can be easily shown that for each $x_0 \geq 0$, $\theta > 0$ and $x \in [0, \theta L(x_0)]$ we have

$$\frac{|L(x_0 + x) - L(x_0)|}{L(x_0)} \leq \theta\lambda(x_0), \quad \frac{|\chi(x_0 + x) - \chi(x_0)|}{\chi(x_0)} \leq \frac{\theta\mu(x_0)}{1 - \theta\lambda(x_0)}, \tag{35}$$

if $\theta\lambda(x_0) < 1$.

The statistical characteristics (L and C) are considered as *slowly changing* along the phase screen coordinate x_0 if the functions $\lambda(x_0)$ and $\zeta(x_0)$ (and then automatically $\mu(x_0) \leq 5\lambda(x_0)/3 + 2\zeta(x_0)$) are sufficiently *small*. The accuracy estimation for (27) depends on parameters $\lambda(t_j)$, $\mu(t_j)$ and θ_j. In particular, by (35), $|L(x_0) - L(t_j)|/L(t_j)$ and $|\chi(x_0) - \chi(t_j)|/\chi(t_j)$ are sufficiently small for all $x_0 \in I_j$ if $\theta_j\lambda(t_j)$ and $\theta_j\mu(t_j)$ are still small enough. Thus the term 'slowly changing statistic characteristics' has 'relative' meaning and indicates that the corresponding relative variation of parameters C_n and L are small within the intervals of length comparable to the turbulence outer scale L).

Consider now the difference

$$\begin{aligned} \left| B_{S_\infty}(x_0, y_0, x_0 + x, y_0 + y) - B_S(x_0, y_0, x_0 + x, y_0 + y) \right| \\ = B_S(x_0, y_0, x_0 + x, y_0 + y) E(x_0, x, y), \end{aligned}$$

which defines the relative error $E(x_0, x, y)$ of the correlation function B_S used in the infinite phase screen generation method described above. From (31)–(35) it follows that, if $\lambda(t_j)$, $\theta_j\lambda(t_j)$, $\mu(t_j)$, $\theta_j\mu(t_j)$ are small enough and $\theta_j \leq \theta_{j+1}$, then for all $x_0 \in I_j$ and $x \in [0, L(x_0)]$ (recall that $r = \sqrt{x^2 + y^2}$) we have

$$\begin{aligned} E(x_0, x, y) \leq \left(2\pi\lambda(t_j)\theta_j + \left(\frac{1}{2} + \frac{3\pi}{4} \right) \mu(t_j) \right) \frac{r}{L(x_0)} \\ + \left(1 + 2\theta_j(\lambda(t_j) + \mu(t_j))\right) \frac{\pi^2}{8\theta_j{}^2} \frac{x^2}{L^2(x_0)}. \end{aligned} \tag{36}$$

In the right hand side of equation (36) we omitted the second-order error terms (comparable to $((\theta_j)^2 + 1)((\lambda(t_j))^2 + (\mu(t_j))^2)$).

The choice of *parameters* θ_j is still in our hands; we just have to follow (to control) the above-mentioned restrictions and satisfy some additional requirements that often arise. In actual applications we can also take into account some specific relationship between the parameters and functions included. Consider the following example, where, in particular, the choice of parameters θ_j is finally presented.

4.3 *An example of phase screen generation with slowly varying statistical characteristics*

In this subsection we are going to show how to find the functions in (34) and to choose parameters θ_j in a variety of concrete situations, and then obtain a direct estimate of $E(x_0, x, y)$. Suppose that the parameter x_0 of the screen S is associated with the altitude $h = h(x_0)$ above the Earth, where $h(x_0)$ is a given positive continuously differentiable function on $[0, +\infty)$. In the commonly used model the parameters l_0, L_0 and $C = AC_n\sqrt{0.066\pi}$ have the following dependence on h

$$L_0 = L(h) = 0.4h, \quad C(h) = c_1 h^{-\omega}, \quad l_0 = l(h) \leq 0.001L(h),$$

where the parameters $c_1 > 0$ and $\omega \in (0, 1)$ are considered as constants on some (rather large) intervals of h (see [31], (1.22) and (1.23)). Note that usually $\omega = 1/3$ or $\omega = 2/3$, dependent on the model used. We assume here that $\omega \in [1/3, 1)$. Since then $L(x_0) = 0.4h(x_0)$ and $C(x_0) = c_1(h(x_0))^{-\omega}$, we have by (28)

$$\chi(\tau) = \chi_0(h(\tau))^{\frac{5-6\omega}{3}}, \quad \frac{|\chi'(\tau)|L(\tau)}{\chi(\tau)} = |5/3 - 2\omega| 0.4h'(\tau),$$

so that, by (34),

$$\lambda(x_0) = 0.4 \sup_{\tau \geq x_0} |h'(\tau)|, \quad \mu(x_0) = \frac{|5 - 6\omega|}{3}\lambda(x_0) \leq \lambda(x_0).$$

In the requirements of and by (36) we obtain for all $x_0 \in I_j$ and $0 \leq r \leq L(x_0)$ (omitting again the second-order smallness error terms)

$$E(x_0, x, y) \leq (2\pi\theta_j + 0.5 + 3\pi/4)\lambda(t_j)\frac{r}{L(x_0)} + (1 + 4\theta_j\lambda(t_j))\frac{\pi^2}{8\theta_j{}^2}\frac{x^2}{L^2(x_0)}. \tag{37}$$

Now, given $\sigma \in (0, 1)$, we want to answer the question: for which ε can we find $\{\theta_j\}$ in such a way that our screen S_∞ becomes (σ, ε)-*precise*, that is $E(x_0, x, y) < \varepsilon$ for all $x_0 \geq 0$ and $x \in [0, \sigma L(x_0)]$? We will suppose that h is non-constant on each interval $[x_0, +\infty)$, $x_0 > 0$. In view of (37), we have to estimate the function

$$E_j(\theta) = (2\pi\theta + 0.5 + 3\pi/4)\lambda(t_j)\sigma + (1 + 4\theta\lambda(t_j))\frac{\pi^2\sigma^2}{8\theta^2}.$$

It can be easily seen that E_j has just one (global) minimum point θ_j^*. By Cardano‘s formula, θ_j^* can be found directly, but we restrict ourselves by the approximation $0 < \theta_j^* - 0.5\sqrt[3]{\pi\sigma/\lambda(t_j)} < 0.357\sqrt[3]{\sigma^2\lambda(t_j)})$. Therefore,

$$\min_{\theta \geq 0} E_j(\theta) \leq E_j^* = 1.5(\pi\sigma)^{4/3}(\lambda(t_j))^{2/3} + (0.5 + 3\pi/4)\sigma\lambda(t_j) + (\pi\sigma)^{5/3}\lambda(t_j)^{4/3}.$$

Since the sequence $\{\lambda(t_j)\}$ is decreasing (see (34)), we have $E_j^* \leq E_0^*$ (where $\lambda(t_0) = \lambda(0)$). So, finally, we can claim that our method works for $\varepsilon \geq E_0^*$. For $\varepsilon = E_0^*$ we take by induction (starting with $t_0 = 0$) $\theta_j = 0.5\sqrt[3]{\pi\sigma/\lambda(t_j)}$. Then $\{\theta_j\}$ is non-decreasing and $\theta_j\lambda(t_j) = 0.5(\pi\sigma\lambda(t_j)^2)^{1/3}$ is small if $\lambda(t_j)$ is. This was in some sense the most precise approximation (where E_j^* are as small as possible for all j) we can obtain with our method. But in this situation we often need to simulate very long screens S_j, which is in fact our initial problem. So, we also present another solution, which looks simpler and reasonable for applications.

Let $\varepsilon \geq E_0^*$. Choose the smallest θ_0 such that $E_0(\theta_0) = \varepsilon$. Since $E_j(\theta_0) \leq E_0(\theta_0)$ we can take $\theta_j = \theta_0$ (all the same!) for $j = 1, 2, \ldots$.

In summary, the generation of an infinitely long phase screen S_∞ on K (with a prescribed slowly changing statistic characteristics) is reduced to the subsequent generation of statistically independent phase screens S_j on rectangles $[-\Delta_{j-1}, \Delta_j]_x \times [-q, q]_y$.

5. Concluding remarks

A conventional approach for long phase screen generation has been too computationally and memory intensive to be practical. In our approach these concerns are essentially mitigated because each computational step requires computation of a relatively small portion of the screen. Specifically, in our algorithm, for the generation of an infinite screen S_∞ on the interval I_j we need to keep in computer memory only generations of two finite screens: S_{j-1} and S_j.

Finally, it is worth mentioning that our 'splicing of screens' algorithm can be used to model two-dimensional random stationary fields of a different nature such as the modeling of random surfaces.

Acknowledgments

The authors are sincerely grateful to V.V. Kolosov for useful discussions. This work was accomplished in the scope of the contract agreement with Sandia National Laboratories (contract no. 243422). Sandia is a multiprogram laboratory operated by Sandia Corporation, a Lockheed Martin Company, for the United States Department of Energy under contract DE–AC04–94AL85000.

References

[1] Ishimaru, A., 1977, *Wave Propagation and Scattering in Random Media* (New York: IEEE Press and Oxford University Press).

[2] Rytov, M. S., Kravtsov, Yu. A., Tatarskii, V. I. and Tatarskii, V. V., 1989, *Principles of Statistical Radiophysics 4, Wave Propagation through Random Media* (Berlin: Springer-Verlag).

[3] Andrews, L. and Phillips, R., 1999, *Laser Beam Propagation Through Random Media* (Bellingham: SPIE Publishing Services).

[4] Fleck, J. A., Morris, J. R. and Feit, M. D., 1976, Time-dependent propagation of high energy laser beams through the atmosphere. *Applied Physics*, **10**, 129–160.

[5] Flatte, S. M., Wang, G. Y. and Martin, J., 1993, Irradiance variance of optical waves through atmospheric turbulence by numerical simulation and comparison with experiment. *Journal Optical Society of America*, **10**, 2363–2370.

[6] Flatte, S. M., 2000, Calculations of wave propagation through statistical random media,with and without a waveguide. *Optics Express*, **10**, 777–804.

[7] Chesnokov, S. S., 1980, Fast Fourier transform in thermal blooming problem. *Vestnik Mav. Fizika, Astronomiya*, **21**, 27–38.

[8] Kandidov, V. P. and Ledenev, V. I., 1981, On application of statistic tests method to the study of wave propagation in nonhomogeneous random media. *Izvestiya Vuzov Radiofizika*, **24**, 438–442.

[9] Kandidov, V. P. and Ledenev, V. I., 1982, Numerical simulation of a refractive index random field in turbulent atmosphere. *Vestnik Mav. Fizika, Astronomiya*, **23**, 3–8.

[10] Konyaev, P. A. and Lukin, V. P., 1985, Thermal distortions of focused laser beams in the atmosphere. *Applied Optics*, **24**, 415–422.

[11] Zuev, V. E., Konyaev, P. A. and Lukin, V. P., 1985, Minimization of atmospheric distortion of optical waves in adaptive optics. *Izvestiya Vuzov Fizika*, **28**, 40–48.

[12] Johnston, R. A. and Lane, R. G., 2000, Modeling scintillation from an aperiodic Kolmogorov phase screen. *Applied Optics*, **39**, 4761–4769.

[13] Lukin, V. P. and Fortes, B. V., 1999, *Investigations of Efficiency for Adaptive Formation of Laser Beams and Images in Turbulent Atmosphere*, Tomsk.

[14] Rytov, S. M., Kravtsov, Yu. A. and Tatarsky, V. I., 1988, *Principles of Statistical Radiophysics* (Berlin. Springer-Verlag).
[15] Kolmogorov, A. N., 1941, A local structure of turbulence in incompressible viscous fluid for very large Reynolds numbers. *Dokladi Akademii Nauk SSSR*, **30**, 299–303.
[16] Obukhov, A. M., 1949, Structure of the temperature field in turbulent flows. *Izvestiya Akademii Nauk SSSR. Geografiya, Geofizika*, **13**, 58–69.
[17] Gurvich, A. S., Kon, A. I., Mironov, B. L. and Khmellevtsov, S. S., 1976, *Laser Radiation in Turbulent Atmosphere* (Moscow: Nauka).
[18] Mironov, V. L., 1981, *Propagation of Laser Beam through the Turbulent Atmosphere* (Novosibirsk: Nauka).
[19] Tatarsky, V. I., 1976, *Laser Radiation in the Turbulent Atmosphere* (Moscow: Nauka).
[20] Vorontsov, M. A. and Shmalhauzen, V. I., 1985, *Principles of Adaptive Optics* (Moscow: Nauka).
[21] Roggemann, M. C. and Welsh, B. M., 1996, *Imaging through Turbulence* (Boca Raton: CRC Press).
[22] Tatarsky, V. I., 1967, *Wave Distribution in the Turbulent Atmosphere* (Moscow: Nauka).
[23] Yaglom, A. M., 1962, *An Introduction to the Theory of Stationary Random Functions* (Englewood Cliffs: Prentice-Hall).
[24] Gihman, I. I. and Skorohod, A. V., 1977, *Introduction to the Theory of Random Processes* (Moscow: Nauka).
[25] Bahvalov, N. S., Zhidkov, N. P. and Kobelkov, G. M., 1987, *Numerical Methods* (Moscow: Nauka).
[26] Gurvich, A. S. and Gracheva, M. E., 1980, Simple model for turbulent fluctuations in optical systems. *Izvestiya Akademii Nauk SSSR. Fizika Atmosferi IOkeana*, **16**, 1107–1111.
[27] Monin, A. S. and Yaglom, A. M., 1965, *Statistical Fluid Mechanics*, Vol. 1 (Moscow: Nauka).
[28] Monin, A. S. and Yaglom, A. M., 1967, *Statistical Fluid Mechanics*, Vol. 2 (Moscow: Nauka).
[29] Watson, G. N., 1922, *Theory of Bessel Functions* (Cambridge: Cambridge University Press).
[30] Sedmak, G., 2004, Implementation of fast-Fourier-transform-based simulations of extra-large atmospheric phase and scintillation screens. *Applied Optics*, **43**, 4527–4538.
[31] Zuev, V. E., Banakh, V. A. and Pokasov, V. V., 1988, *Optics of the Turbulent Atmosphere*, Gidrometeoizdat.